Applied Catalysis A: General 532 (2017) 65–76

Contents lists available at ScienceDirect

Applied Catalysis A: General

journal homepage: www.elsevier.com/locate/apcata

Oxidative coupling of methane on Sr/La_2O_3 catalysts: Improving the catalytic performance using cordierite monoliths and ceramic foams as structured substrates

Brenda M. Sollier, Leticia E. Gómez, Alicia V. Boix, Eduardo E. Miró*

Instituto de Investigaciones en Catálisis y Petroquímica, INCAPE (FIQ, UNL-CONICET), 3000 Santa Fe, Argentina

ARTICLE INFO

Article history:
Received 30 August 2016
Received in revised form
14 November 2016
Accepted 19 December 2016
Available online 21 December 2016

Keywords:
Structured catalysts
Oxidative coupling of methane
Sr/La_2O_3 catalyst
Monoliths and foams

ABSTRACT

This work shows how the use of structured catalysts results in an important increase of the C_2 yield in the oxidative coupling of methane over Sr/La_2O_3 catalysts. Solids with 2 and 5 wt.% of Sr (Sr2 and Sr5) were prepared and washcoated on cordierite monoliths and alumina foams. Homogeneous and mechanically stable catalytic films were obtained in both cases with the addition of silica as binder. Other types of foams were also prepared (aluminum silicate and magnesia stabilized zirconia) but in such cases the adhesion of coatings was rather poor. The catalytic surface XPS characterization of both powders and structured catalysts indicates that lanthanum is mainly present as hydroxide and carbonate and that strontium is mainly present as carbonate. However, in the case of washcoated cordierite monoliths, a modification in La 3d spectra measured by XPS suggests a strong interaction of La with its chemical environment, most probably with silica and/or magnesia. This interaction could be originated by migration of the cordierite components towards the catalytic film, as seen by EDX. The decomposition of $La(OH)_3$ and $La_2O_2CO_3$ into La_2O_3 under reaction conditions was confirmed by in situ LRS. While hydroxide prevails at low temperature, the presence of oxycarbonates starts to be relevant when the reaction takes place at temperatures above 400 °C and the oxycarbonates decompose into oxide over 700 °C. The monolithic catalysts (M)Sr2 and (M)Sr5 resulted twofold more active towards ethane and ethylene than the corresponding Sr2 and Sr5 powders. Meanwhile, the washcoated alumina foam (FAl)Sr5 showed methane conversion values similar to those of the powder but higher C_2 selectivity; thus, the C_2 yield was also higher. In the case of the monolithic catalysts, the increase in methane conversion and C_2 yield could be related to the interaction of Sr and La with silica and/or magnesia present in the cordierite structure. In the case of the alumina foam catalyst, the higher selectivity could be originated by the lower gas phase/catalytic surface ratio (as compared with the monolith), that inhibits gas-phase combustion of C_2 products. In order to assess the stability of (M)Sr5, which was the best catalyst among the ones studied in this work, time-on stream runs at 600 and 800 °C were performed. Surprisingly, at 800 °C, the C_2 yield steeply increased from 18% to 22.5% during the first 70 h and then remained constant until 100 h. This phenomenon could be due to a gradual increase in chemical interactions between the cordierite components and the catalytic coat. At lower temperature (600 °C), C_2 yield was constant during the 100 h of time-on-stream, indicating that this temperature is not enough to produce the said effect.

1. Introduction

Natural gas is an energy source that has been gaining attention in the last few years due to the development of new fracking methods. Shale gas deposits are distributed across the globe, mainly in Asia, Europe, North and Latin America, China and Argentina being the countries with the largest reserves [1]. Therefore, conversion of methane, one of the main components of natural gas into ethane and ethylene via the oxidative coupling of methane (OCM) has renewed its importance [2,3].

The OCM reaction was first reported by Keller and Bahsin [4]. In their work, they demonstrated that this reaction proceeds in more favorable thermodynamic conditions than direct methane conversion. The OCM reaction is produced by oxidative dehydrogenation

* Corresponding author.
E-mail addresses: emiro@fiq.unl.edu.ar, cabemiro@hotmail.com (E.E. Miró).

http://dx.doi.org/10.1016/j.apcata.2016.12.018
0926-860X/

of methane molecules through methyl radicals. These radicals couple with each other to form ethane and ethylene [5].

During the 90s, despite the research efforts devoted to the OCM reaction, no acceptable yield was accomplished to justify its industrial application. However, some important conclusions were academically achieved about the reaction mechanism and active catalyst sites [6]. In this way, methane dehydrogenation and methyl radical coupling were considered as the clue reaction steps [7].

As said before, in the last few years, the interest in the OCM reaction has increased and catalysts with higher activity and selectivity have been found [8,9]. In this way, with oxides as MgO, MnO_2, and La_2O_3, acceptable reaction performances have been reached. These oxides could be promoted by basic compounds like Li, Na and Sr that can contribute to generate superficial active sites for methane dehydrogenation [10–13].

It is noteworthy that the OCM reaction is highly exothermic and hot spots are easily produced in the reactor [7,8]. Thus, the development of non-conventional reactors to optimize heat and mass transfer processes should be taken into account [14–16]. These aspects are related to process fluid dynamics; in fact, the importance of the relationship between gas-phase and surface reactions was reported several years ago by Lane and Wolf [5].

Monolithic catalysts could be a good option to deal with the challenges described above. This type of structure has a lower pressure drop, smaller diffusion resistance and better mass and heat transfer than powder catalysts. Cordierite is the most widely used material for honeycomb manufacturing given its superior hydrothermal stability, mechanical features and low thermal expansion coefficients [17]. Ceramic foams represent another attractive alternative for structured systems that can be prepared from a range of materials, such as alumina, silicon carbide, aluminum silicates and zirconium silicates. Their properties make them excellent substrates [18]. For example, ceramic foams exhibit high porosities with a significant interconnectivity, which results in low pressure drop. In both structures, monoliths and foams, good contact between gas phase and surface reactions is achieved. The catalytic film incorporation to these structures can be performed by different techniques, washcoating being the one most commonly used [19].

In this study, the working hypothesis consists in taking advantage of the beneficial properties of monoliths and foams in order to support an active catalyst for the OCM reaction, with the aim to foresee the feasibility of its application in real conditions. For the preparation of structured catalysts, we selected Sr/La_2O_3 as the active phase taking into account a statistical analysis of the literature performed by Kondratenko et al., in which the authors concluded that Sr is the best dopant for the host metal oxides La_2O_3 and MgO [20]. In this vein, promising Sr/La_2O_3 structured catalysts to be used in the OCM reaction are presented in this work.

Cordierite monoliths, alumina, aluminum silicate and zirconium oxides foams were used as substrates for the preparation of structured catalysts [21–23]. Firstly, two Sr/La_2O_3 catalysts with different Sr content (2 and 5%) were prepared in order to study the strontium loading influence on the OCM reaction. Then, the active phase was added to the support by the washcoating technique. Two different synthesis methods were studied for cordierite monolithic catalysts: sequential La_2O_3 and Sr loading, and washcoating from a slurry made of Sr/La_2O_3. This latter method was used to coat foam structures with the Sr/La_2O_3 slurry.

In addition to the activity and stability studies of the catalysts prepared, their physicochemical properties were also studied using a battery of techniques. The structured catalysts were inspected by scanning electron microscopy (SEM) in order to analyze the morphological characteristics of the films deposited onto the structures; chemical mapping was studied using Energy-dispersive X-ray spectroscopy (EDX), and the mechanical stability of coatings was analyzed using an ultrasound test. Structured and powder catalysts were also characterized by X-ray Photoelectron Spectroscopy (XPS) and Laser Raman Spectroscopy (LRS). In situ Laser Raman Spectroscopy was used to characterize catalysts under reaction conditions.

2. Experimental

2.1. Catalysts preparation

2.1.1. Powder catalysts preparation

In order to deposit the catalysts onto cordierite, two powders were prepared by wet impregnation [17]. A commercial La_2O_3 (Alfa Aeser, 99.9%) powder was mixed with an aqueous solution of $Sr(NO_3)_2$ (Sigma Aldrich, 99.9%) and the water was evaporated under continuous stirring during 4 h at 80 °C until a paste was obtained. Then, this paste was placed in an oven at 150 °C overnight. After drying, the samples were calcined for 10 h at 850 °C under air. Powder catalysts with 2 and 5 wt.% strontium over lanthanum oxide were denoted as Sr2 and Sr5, respectively.

2.1.2. Monolithic catalysts preparation

Cordierite honeycomb monoliths (Corning, 400 cpi, 0.1 mm wall thickness) were used as substrates. The supports were cut in an average size of 1 cm × 1 cm and 2 cm length as shown in Fig. 1(A). As a cleaning procedure, cordierite pieces were washed in ultrasonic bath (Cole Parmer, 47 kHz and 130 W) with acetone during 30 min and then with distilled water. The monolithic catalysts were obtained by two different methods.

The first method was based in the deposition of La_2O_3 onto cordierite monolith by washcoating and the subsequent strontium incorporation. This procedure consisted in immersing the substrates during 30 s in 20 cm^3 of La_2O_3 slurry. The slurry was prepared in distilled water with a solid concentration of 20 wt.%. Also, 1 wt.% of colloidal silica was added to improve adherence. After each immersion, the pieces were blown with air in order to remove the slurry excess during 10 s and then they were dried at 120 °C for 90 min. This immersion-blowing-drying cycle was repeated as many times as necessary to achieve the desired lanthanum oxide loading. Then, the samples were calcined at 850 °C during 4 h and after that, strontium was incorporated by impregnation with an aqueous solution containing 0.43 M of $Sr(NO_3)_2$. The monolith coated with La_2O_3 was immersed in 20 cm^3 of the strontium solution during 30 s, the solution excess was blown for 10 s and the monolith was dried at 120 °C during 90 min, calcined at 850 °C during 4 h, and weighted. This procedure was repeated several times until the desired Sr loadings were achieved (2 or 5 wt.% of Sr). These catalysts were denoted as (M)Sr2S and (M)Sr5S, respectively.

The second preparation method was based on the deposition of the catalysts previously prepared (Sr2 or Sr5) onto cordierite honeycomb monoliths following the same immersion-blowing-drying procedure described in the first method for deposition of the film. Two different slurries were prepared in order to incorporate the catalysts, 20 wt.% Sr2 or 20 wt.% Sr5, with 1% of silica. Finally, the samples were calcined at 850 °C for 4 h. The catalysts were denoted as (M)Sr2, prepared from Sr2 slurry, and (M)Sr5, from Sr5 slurry.

2.1.3. Catalytic ceramic foams preparation

Ceramic foams based on magnesia-stabilized zirconia, aluminum silicate and alumina foams were also studied as substrates in this work. The first two foams were provided by Medemet, and the pictures are shown in Fig. 1(B) and (C), respectively. The samples were cut in the same average size as monoliths. The preparation method was identical as the second method presented in the cordierite honeycomb monoliths. An aqueous solution of 20 wt.%

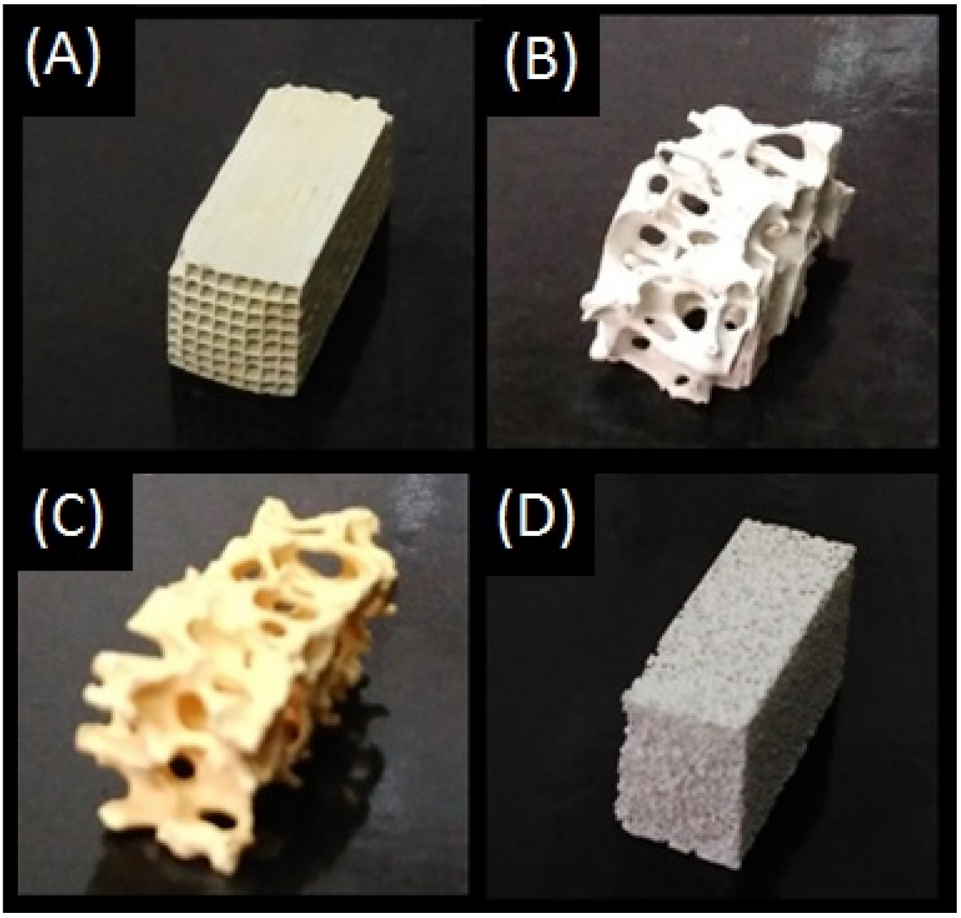

Fig. 1. Images of the different structures: (A) Cordierite monolith, (B) Aluminum silicate foam, (C) Magnesia-stabilized zirconia foam and (D) Alumina foam.

Sr5 with 1 wt.% of silica was prepared and the pieces were wash-coated into this solution with the immersion-blowing-drying cycle previously described. The sample containing Sr5 coated into aluminum silicate foam was denoted as (FSiAl)Sr5 after calcination at 850 °C during 4 h. The other catalyst also containing Sr5 coated into magnesia-stabilized zirconia foam was denoted as (FZr)Sr5 after calcination at 850 °C during 4 h.

The third foam studied in this work was alumina foam (Good Fellow, 86% porosity, 26 pores/cm); the structure is also included in Fig. 1(D). The preparation method was similar to the previous one but, because this foam's hollows are considerably smaller than those previously described, the immersion step was carried out under vacuum in order to assure thorough contact of the structure with the 20 wt.% Sr5 slurry. This sample was denoted as (FAl)Sr5 after calcination.

2.2. Mechanical stability test

The coating stability test was performed with each structured catalyst previously calcined in order to evaluate the adherence of the catalytic coatings. The coated monoliths and foams were immersed in acetone inside a glass vessel which was then placed in an ultrasonic bath during 5 min (Cole Parmer, 47 kHz and 130 W). The samples were dried in an oven at 120 °C for 1 h. The sequence was repeated several times until the weight loss stayed stable. The weight was measured after and before each cycle. Finally, the adherence percentage was referred to the added catalytic layer.

2.3. Catalysts characterization

2.3.1. Scanning electron microscopy (SEM)

The morphology of the catalytic coatings was examined with a scanning electron microscope SEM, JEOL JSM-35C operated at 20 kV acceleration voltage. Pieces of different samples were observed in order to study the inner channel walls and cross-sections. The portions were glued to the sample holder with Ag painting and then coated with a gold thin layer in order to improve the images obtained.

2.3.2. Chemical mapping using energy-dispersive X-ray analysis (EDX)

The elemental chemical analysis was performed using a Phenom ProX microscope with a fully integrated EDS detector and software. Results were obtained by the theoretical quantitative method (SEMIQ) which does not require standards. The distribution of the different elements in the catalytic layer was evaluated with the Element Identification (EID) software package and a specially designed and fully integrated Energy Dispersive Spectrometer (EDS). The apparatus was equipped with a Silicon Drift Detector Thermoelectrically cooled (LN_2 free). Samples were studied using a charge reduction sample holder with no need to coat them.

2.3.3. X-ray photoelectron spectroscopy (XPS)

XPS analyses were performed in a multi-technique system (SPECS) equipped with a dual Mg/Al X-ray source and a PHOIBOS 150 analyzer operating in the fixed analyzer transmission (FAT) mode. The spectra were obtained with pass energy of 30 eV; the Al Kα X-ray source was operated at 200 W and 12 kV. The working

pressure in the analyzing chamber was less than 4.5×10^{-9} torr. The XPS analyses were performed on the calcined catalysts. The spectral regions corresponding to Sr 3d, O 1s, La 3d, Mg 2p, Al 2p, Si 2p and C 1 s (reference B.E. 284.6 eV) core levels were recorded for each sample. The data treatment was performed with Casa XPS program (Casa Software Ltda., UK). Peaks were considered to be a mixture of Gaussian and Lorentzian functions in a 70/30 ratio. The ratio of La $3d_{5/2}$ and La $3d_{3/2}$ peaks area was fixed to 3:2.

2.3.4. Laser Raman spectroscopy (LRS)

Structured catalysts and powders were characterized by means of a Horiba JOBIN YVON Lab RAM HR instrument. The excitation source was the 514.5 nm line of Spectra 9000 Photometrics Ar ion laser with its power set at 30 mW.

The Sr5 powder catalyst was studied by in situ Raman Spectroscopy under reaction conditions using a Linkam high temperature cell. The powder catalyst was placed into the reaction camera and the gas feed flowed through the solids. The feed mixtures were prepared in a flow system built for this purpose. The Sr5 catalyst was exposed to reaction conditions at temperatures between 25 and 600 °C.

2.4. Catalytic test

The experiments were conducted in a fixed-bed flow quartz reactor at atmospheric pressure. The reactant flow entered the reactor through an inner section of 16 mm diameter, but below the catalyst bed this inner section was reduced up to 1/8 inch diameter in order to decrease the homogeneous combustion of hydrocarbon products as much as possible. The reactor was heated with a furnace to reach the desired temperatures. The exiting gases from the reactor were conducted through a condenser in order to eliminate H_2O from the flow.

Unreacted methane, coupling products and byproducts were measured using gas chromatograph (GC-2014 Shimadzu) with a thermal conductivity detector (TCD) equipped with two columns, Zeolite 5A and Hayesep D. The carbon balance was better than 97%.

The reaction mixture consisted of 64% CH_4, 8% O_2 and 28% He. The catalyst weigh/total flow ratio was 0.166 mg cm^{-3} min.

Although only above 600 °C methane conversions obtained were higher than 20%, the catalysts were tested in a wide temperature range (300–800 °C). Methane conversion (X_{CH4}), C_2 selectivity (S_{c2}) and C_2 yield (y_{c2}) were calculated as follows:

$$X_{CH_4}(\%) = \frac{[CH_4]^0 - [CH_4]}{CH_4{}^0} \times 100$$

$$S_{C_2}(\%) = \frac{2([C_2H_4] + [C_2H_6])}{[CH_4]^0 - [CH_4]} \times 100$$

$$y_{c_2}(\%) = X_{CH_4} \times S_{C_2} \times \frac{1}{100}$$

Where:

$[CH_4]^0$: initial methane concentration.

$[CH_4]$: methane concentration at the reactor exit.

$[C_2H_4]$: ethylene concentration at the reactor exit.

$[C_2H_6]$: ethane concentration at the reactor exit.

The stability of the monolithic catalyst (M)Sr5 was studied by two time-on-stream runs performed during 100 h, one at 600 °C and the other at 800 °C.

Since the reaction under study is exothermic, the axial temperature profile along (M)Sr5 monolith was determined under reaction conditions at 800 °C, in order to analyze the possible formation of a severe hot spot. This was done by fixing the oven power to ensure a temperature of 800 °C at the center of the monolith and moving the reading thermocouple (1 mm diameter) along several positions inside the monolith channel, in a way similar to the experiment performed by Sanz et al. [24]. In order to ensure the thermocouple inside the channels, one center channel wall (one of 256) was removed and the instrument was placed inside the hole between two channels.

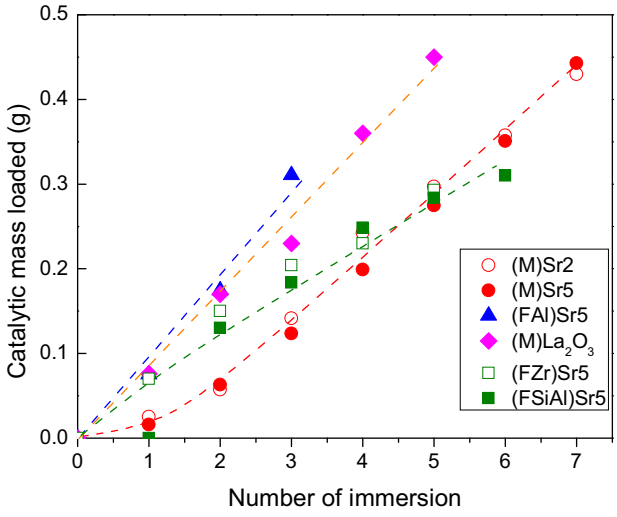

Fig. 2. Evolution of the catalytic loaded mass after sequential impregnations of the different structured catalysts studied.

3. Results and discussion

3.1. Structured catalysts preparation

In order to compare the catalytic behaviors between powders and structured catalysts, the same value of *catalytic mass/total gaseous flow* ratio (W/F) was used. For this purpose, between 400 and 500 mg of catalyst were washcoated into the cordierite monolith pieces, for which between 5–7 immersion – blowing – drying cycles were required. Two different preparation methods were performed, La_2O_3 washcoating followed by Sr impregnation, and washcoating of the ready-made Sr2 or Sr5 catalysts. In Fig. 2, the loaded catalytic mass vs. immersion number is presented for the different substrates. In the case of the first method, 5 cycles were needed to gain 400 mg of La_2O_3 into the monolith (denoted as (M)La_2O_3 in Fig. 2). Afterwards, Sr was incorporated by several immersions in an aqueous solution of strontium nitrate in order to reach 2 or 5 wt.%. When Sr2 or Sr5 catalytic powder was added to monoliths, 7 cycles were required to obtain approximately the same catalyst loading (400 mg).

Loaded mass vs number of immersions for the three different foams are also shown in Fig. 2. The mass gained in these cases was 300 mg because of the characteristic substrate building. Foams have interconnected pores and over 300 mg of catalyst could block the structure and interfere in the desired gas flow through the holes during reaction. Only 3 cycles were needed to achieve 300 mg of catalyst in the case of alumina foams, (FAl)Sr5, while for the other foams, (FSiAl)Sr5 and (FZr)Sr5, the adherence was weaker and 5 cycles were needed.

Stability test results of the film coatings into the structures are shown in Fig. 3. The weight loss of (M)Sr2 and (M)Sr5 is presented. In both cases, it was less than 6% while for monoliths coated with La_2O_3 film, weight loss was around 12%. The good adherence reached could be due to monolith macropores, in which lanthanum oxide particles (12 μm approximately) remained attached to the

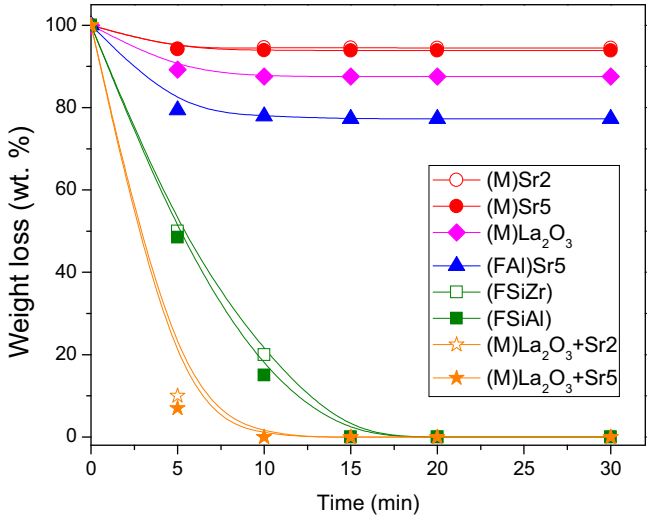

Fig. 3. Mechanical stability test of catalytic films.

structure. The addition of colloidal silica as binder also improved adherence, without this binder the weight loss was over 80%.

The worst stability test results were shown by cordierite monoliths prepared by sequential impregnation. The (M)Sr2S and (M)Sr5S catalysts showed a weight loss of 100% after 10 min of ultrasonic treatment. This poor adherence could be attributed to the slightly acid pH of the $Sr(NO_3)_2$ solution that could weaken La_2O_3 film previously attached to monolith walls. Furthermore, the La_2O_3 film could easily hydrate to produce hydroxide, and it could also form carbonate and oxycarbonate when in contact with ambient CO_2.

On the other hand, (FAl)Sr5 exhibited a total weight loss close to 25%, while the other two foams, (FSiAl)Sr5 and (FZr)Sr5, exhibited a 100% weight loss after 15 min of treatment.

3.2. Catalytic coatings morphology and EDX results

The (M)Sr5 coating morphology is shown in Fig. 4. Images (A)–(D) show different regions from selected monolith channels cross-sections. It can be observed that the catalyst coating morphology is homogeneous on the channel walls. It can be noticed that coatings show high porosity and the monolith wall is fully covered with the catalyst (Fig. 4(A) and (B)). In Fig. 4(C), it can be seen that the layer was thicker at the corners of the square cells. This difference in thickness is caused by the fluid dynamic phenomena during the blowing step of the Sr5 deposition procedure. In Fig. 4(D), it is shown that catalyst particles penetrated through the cordierite macropores and their interconnections during the immersion step. This could explain the good adherence that these catalysts presented. (M)Sr2 did not show significant differences with (M)Sr5.

Fig. 4(E) shows a linear scan of the different elements present in a cross-section cut of a channel wall of (M)Sr5 structured catalyst by EDX technique. If La distribution is followed, it could be clearly seen that inside cordierite, the average lanthanum concentration is low. Nevertheless, as said above, SEM images show that La_2O_3 is present inside the macroporous, thus allowing the anchorage of the washcoat. In the catalytic film, lanthanum concentration increases, being the highest one among all the elements (except for oxygen). On the other hand, when the distribution of the oxides present in the cordierite structure (SiO_2-MgO-Al_2O_3) is studied, it is clear that they migrate towards catalytic film. For example, MgO has a homogeneous distribution into cordierite until the interface with the catalytic film. From that point, its concentration decreases, but it can be clearly observed that, to some extent, it is present in the active film. The same behavior is shown by Al_2O_3 and SiO_2. Noticeably, Sr distribution is clearly homogeneous in both zones. Since strontium is believed to be responsible for the generation of vacancies into the host oxides [25–27], the homogeneous distribution into cordierite and film suggests that there are active sites dispersed in the totality of the catalyst (film and structured support). Finally, oxygen distribution is in agreement with the metal/oxygen ratios of each oxide into the profile line analyzed.

From what is said above, it can be concluded that Sr is in intimate contact not only with La_2O_3 but also with cordierite oxides; and that MgO, Al_2O_3 and SiO_2, the main components of cordierite, are also present in the catalytic coating. Thus, a complex mixture of oxides is generated due to the migration of the different components during calcination at 850 °C.

Fig. 5 shows bare Al_2O_3 foam (A and C) and (FAl)Sr5 foam (B and D). If both pairs of figures are compared, it could be clearly seen that the alumina foam is fully covered by the catalytic film. In addition, it presents high substrate porosity and homogeneous cover morphology. An elemental mapping by EDX was also performed over (FAl)Sr5 (not shown) in which migration of aluminum from the foam structure to the catalytic film was not observed. Thus, despite the fact that lanthanum is well dispersed into the alumina foam porosity, as seen by SEM, the interaction of the foam with the washcoat is low, which could explain why adherence is poorer than that of (M)Sr5.

Fig. 6(A)–(C) show (FSiAl)Sr5 micrographs and (D) to (F) (FZr)Sr5 micrographs. In (A) and (D), the foam surface is shown, without coating. The roughness of the material can also be observed. Moreover, in (C) and (F) it can be noted that these structures have bigger holes than the ones seen in the alumina foam. Noticeably, film morphology is not homogeneous, exhibiting agglomeration and some line fractures.

3.3. XPS results

The chemical nature of the species present on powder and structured catalysts surface can be studied by XPS. The La 3d spectrum of Sr5 powder catalyst consists of two main peaks belonging to La $3d_{5/2}$ and La $3d_{3/2}$ split, and their respective satellite peaks (Fig. 7(A)). The La $3d_{5/2}$ core level is observed at 835.4 eV (fwhm 2.8 eV) and its corresponding satellite at +3.5 eV (Table 1). Both lanthanum species, La_2O_3 and $La(OH)_3$, have close binding energy values [28,29]. Sunding et al. reported La $3d_{5/2}$ values of 834.9 eV for La_2O_3 and 835.1 eV for $La(OH)_3$ [30]. In addition, the ratio between satellite and main peak intensities was calculated and it resulted 0.77-0.78 (Table 1), which could be associated to the $La(OH)_3$ phase. Similar results were obtained for Sr2 and Sr5 + SiO_2 powders. This latter sample was prepared as Sr5 but with the addition of 1% SiO_2 during wet impregnation in order to compare with the washcoating slurry.

Binding Energy values of La 3d measured for structured catalysts did not show significant differences with respect to powders. However, a noticeable widening of main and satellite peaks was observed, the fwhm approximately increasing from 2.7 to 4.0 eV (main peaks) and from 2.9 to 3.8 eV (satellite peaks). Also, satellite/main peaks intensity ratio was close to 0.77 for powders and foam catalysts, and around 0.95 for monoliths (Table 1). The satellite peak intensity increase observed in monoliths was attributed to a possible interaction with the cordierite during the calcination step at high temperature (850 °C). This observation is in agreement with that made in section 3.2. according to the EDX mapping, the cordierite components SiO_2-MgO-Al_2O_3 migrated into the catalytic film, thus an interaction between the catalytic phase and the said compounds could have occurred. In this vein, the reaction between La_2O_3 with SiO_2 to form $La_2Si_2O_7$ has already been reported, yield-

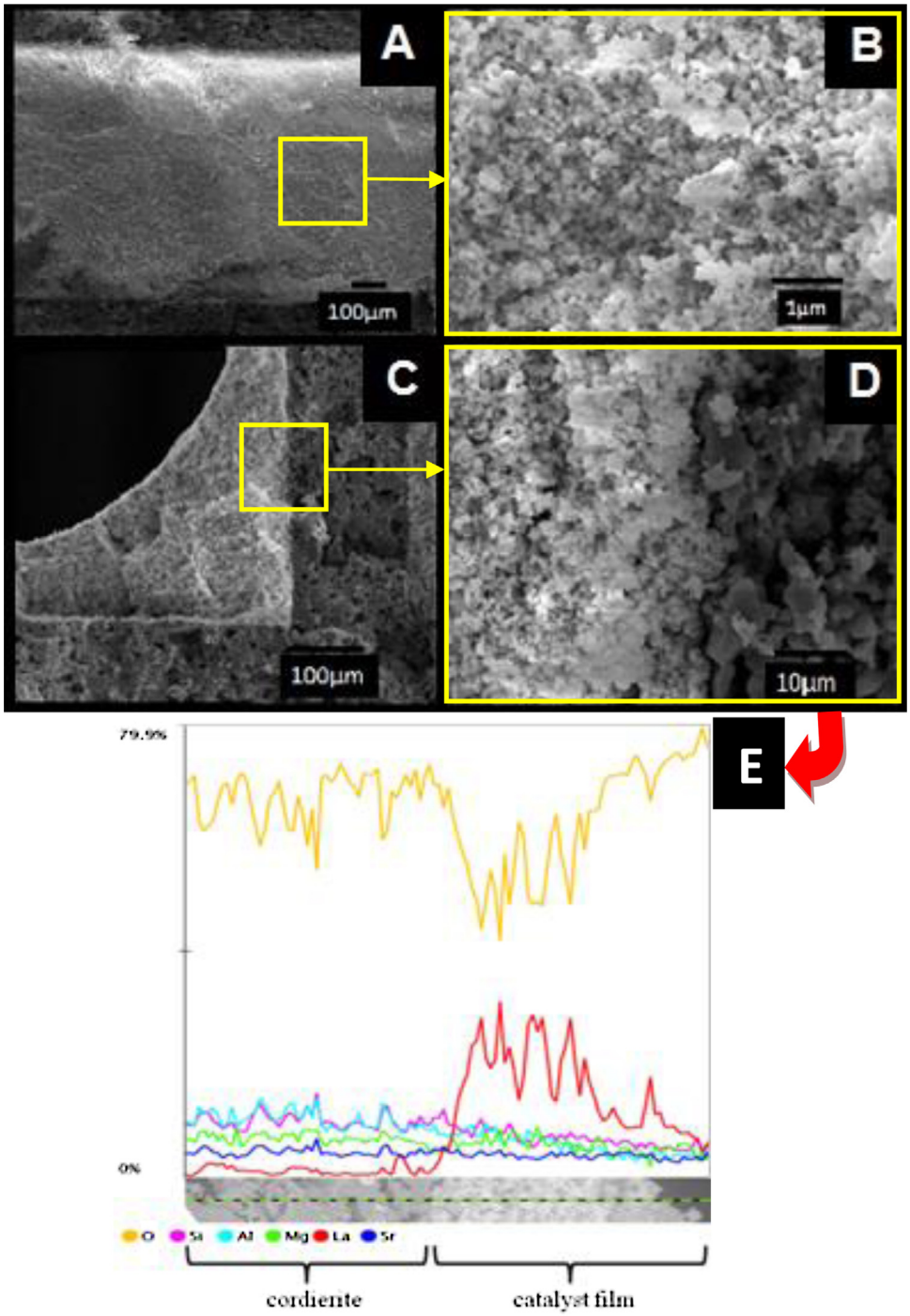

Fig. 4. SEM photomicrographs of (M)Sr5 catalyst. (A) Monolith channel top view, (B) monolith channel top view magnification, (C) monolith cross section, channel frontal view, (D) monolith cross section, channel frontal view magnification and (E) EDX linear scan over the zone depicted in (D).

ing a spectrum similar to the one presented in Fig. 7(A) [29,31,32]. However, the interactions with alumina and magnesium oxide compounds should not be discarded. In the case of the mixture of lanthanum oxide with silica (1 wt.%, as the binder) the spectrum does not show any difference if compared with pure La_2O_3, probably because the low silica amount was not enough to produce this phenomenon.

Fig. 7(B) shows the O 1 s spectra corresponding to Sr5, (M)Sr5 and (FAl)Sr5. In this region three peaks appear at 530.1, 531.6 and 533.1 eV (Table 1) over Sr5 catalyst. The peak at lower binding energy corresponds to lattice oxygen (O^{2-}) and it represents 8% of the total oxygen, whereas the one at 531.6 eV could be attributed to a mixture of different species, including hydroxyl (OH^-), carbonate (CO_3^{2-}) and peroxide ion (O^-), all with similar BEs. This peak is the oxygenís main component with a concentration of 50%. The latter peak at 533.1 eV could come from residual molecular water adsorbed in the catalyst or from the superoxide species (O_2^-); it represents 42% of total oxygen. An experiment was performed in order to eliminate residual water from the catalyst surface. Sr5 was calcined at 850 °C during 10 h and immediately then, it was placed into the XPS chamber and a pretreatment at 200 °C under vacuum (6×10^{-3} Pa) was performed. Surprisingly, this peak was

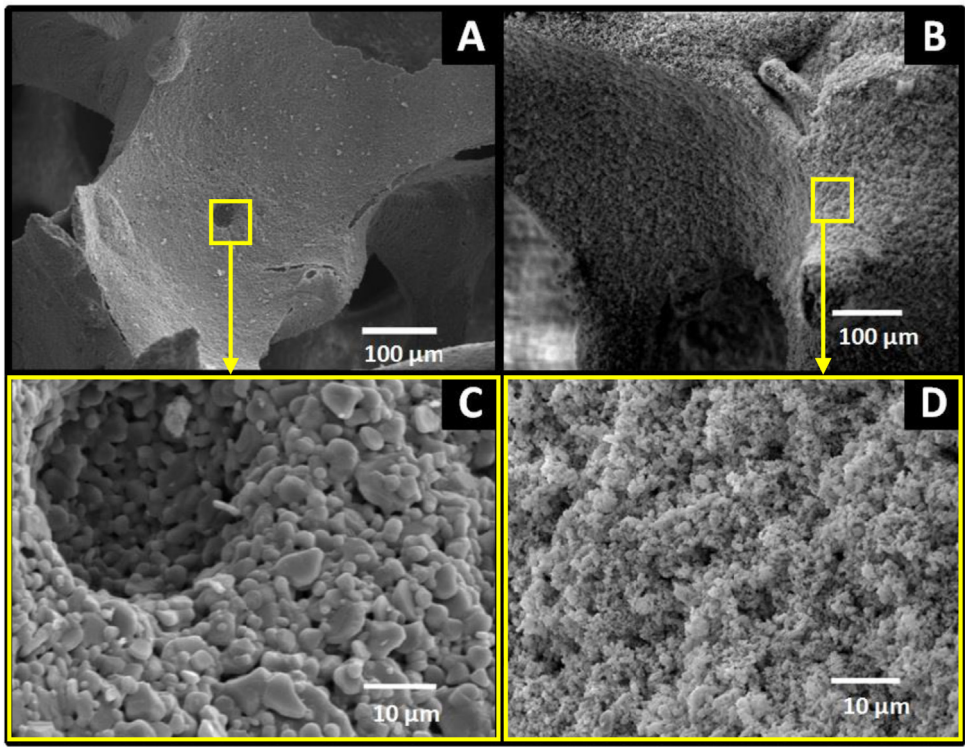

Fig. 5. SEM photomicrographs. (A) and (C) bare Al_2O_3 foam with different magnification, and (B) and (D) coated (FAl)Sr5 with different magnification.

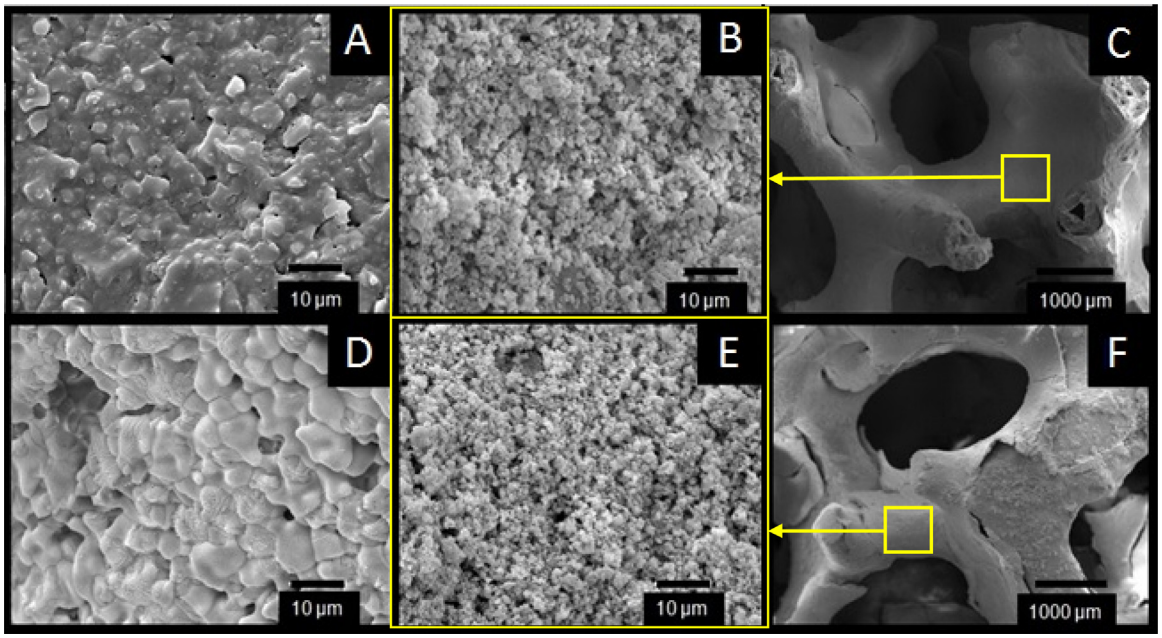

Fig. 6. SEM photomicrographs of: (A) (FSiAl) bare foam, (B), (C) coated (FSiAl)Sr5 with different magnification, (D) (FZr) bare foam, (E), (F) coated (FZr)Sr5 with different magnification.

still present into the O 1 s XPS spectra. That indicates that the peak at 533.1 eV would correspond to superoxide species. Islam et al. investigated the formation of peroxide and superoxide species, as these were supposed to be responsible for methane activation during OCM reaction on this material [33]. It is believed that electron deficient species such as O^- and O_2^- on the catalysts surface are effective for increasing C_2 selectivity [9,34].

A similar behavior was observed in the other two powders, Sr2 and Sr5 + SiO_2 (Table 1). On the other hand, only two peaks appeared at around 530.7 and 532.0 eV on the structured catalysts surface. The peak at lower binding energy was assigned to lattice oxygen (more than 60% of total oxygen) and the one at highest binding energy, to the peroxide ion (O^-), OH^- and CO_3^{2-} oxygen species [35]. The higher amount of lattice oxygen could be attributed to the contribution of SiO_2, Al_2O_3 and MgO present on the surface. As it was already discussed, these components migrate to the catalytic film modifying the original surface composition.

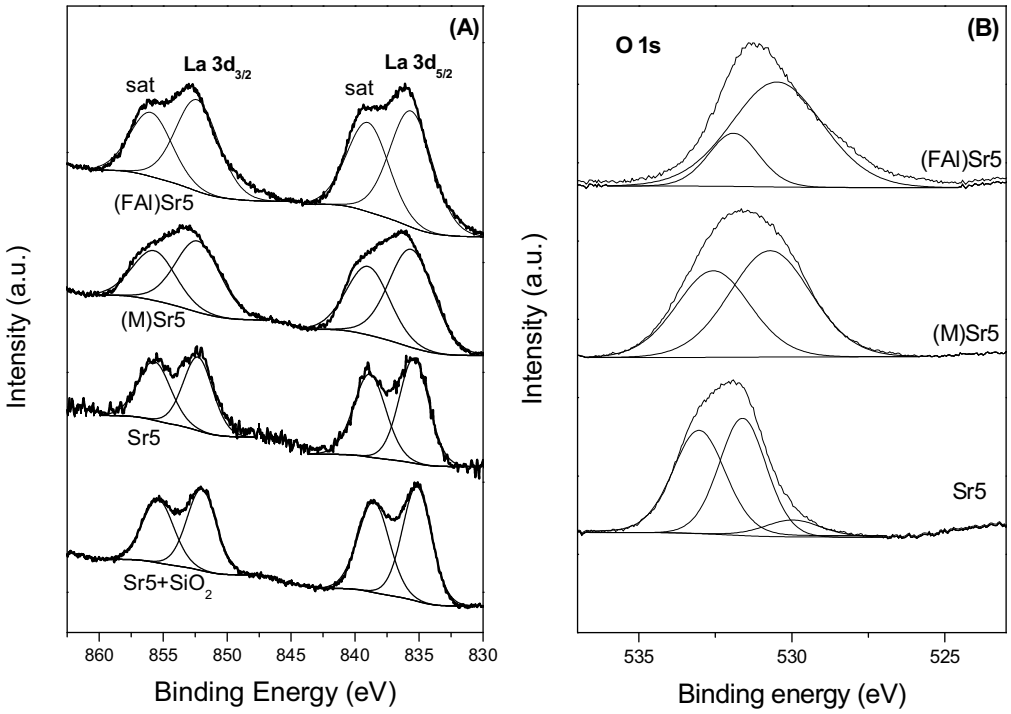

Fig. 7. XPS results. (A) La 3d spectra and (B) O 1 s spectra.

Table 1
XPS results.

Sample	Binding Energy (FWHM)/eV			I_{sat}/I_{mp}[b]	$Sr/La)_{surface}$
	O 1s	La $3d_{5/2}$	Satellite[a]		
Sr2	530.5(3.3)/12[c] 531.6 (2.0)/57 533.1 (1.8)/31	835.4 (2.8)	838.9 (2.9)	0.77	0.43
Sr5	530.1 (2.9)/8 531.6 (1.9)/50 533.1 (2.0)/42	835.4 (2.7)	838.9 (2.9)	0.78	0.56
$Sr5+SiO_2$	530.1 (3.5)/8 531.4 (2.3)/74 532.9 (2.3)/18	835.4 (2.7)	838.5 (2.9)	0.77	0.55
(FAl)Sr5	530.5 (3.5)/78 531.9 (1.9)/22	835.6 (3.9)	839.0 (3.7)	0.77	0.52
(M)Sr2	530.7 (3.4)/73 532.3 (2.6)/27	835.5 (4.1)	838.9 (3.8)	0.95	0.26
(M)Sr5	530.7 (3.1)/58 532.6 (2.8)/42	835.5 (4.1)	838.9 (3.9)	0.96	0.39

[a] Corresponding to La $3d_{5/2}$ core level.
[b] Satellite/main peak intensity ratio for La $3d_{5/2}$.
[c] Percentage fraction of each oxygen component.

The Sr 3d spectra present a peak at 133.8–134.2 eV in all catalysts, which corresponds to $SrCO_3$ species [9,36]. The Sr/La surface atomic ratio changes with the amount of Sr added to the catalyst and the values are higher than theoretical Sr/La bulk ratio. This is caused by the synthesis method in which Sr is impregnated on the La_2O_3 surface. For Sr2, this value is 0.43 and for the catalysts with 5 wt.% Sr, the Sr/La ratio is around 0.5 (Table 1). However, in the case of monoliths the values are lower than in powders and foam, 0.26 for (M)Sr2 and 0.39 for (M)Sr5. This decrease is related to the diffusion of the Sr into the cordierite support as seen by EDX. It confirms the homogenous dispersion of strontium into the totality of the catalyst structure.

In addition, the presence of Mg, Al and Si (cordierite main components) was detected on (M)Sr5 surface. The values of Mg/La, Al/La and Si/La resulted 0.34, 0.65 and 0.06, respectively. Another important fact that could be concluded by these results is that Al diffusion is considerably lesser than that of Mg and Si.

In C 1 s region, there appeared a peak at 288.0 eV and it corresponds to CO_3^{2-} species. This is in agreement with the species observed in the O 1 s region.

3.4. Laser Raman spectroscopy characterization

Laser Raman Spectra of Sr2 and Sr5 powder catalysts and (FAl)Sr5, (M)Sr2 and (M)Sr5 structured catalysts are shown in Fig. 8. In the case of the two powders, six bands at 140, 226, 287, 343, 453 and 603 cm^{-1} are observed. These bands correspond to those reported for the crystalline $La(OH)_3$ phase [37]. In addition, two weak signals at 179 and 397 can be observed which could be

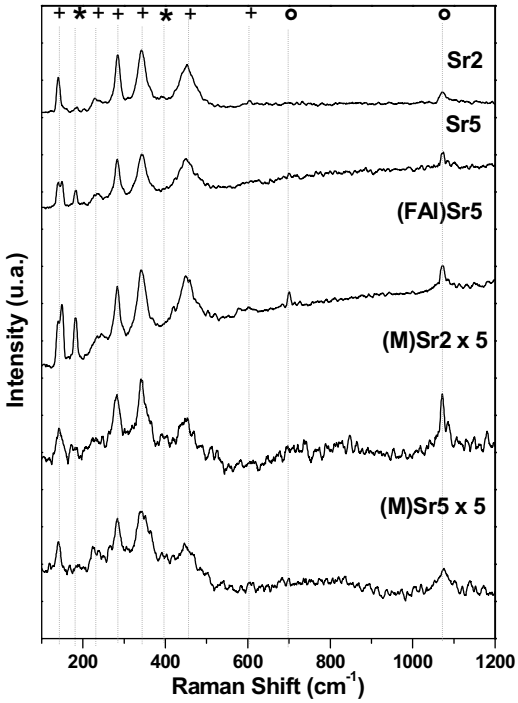

Fig. 8. LRS results of powder and structured catalysts (+$La(OH)_3$, * La_2O_3, ° $La_2O_2CO_3$).

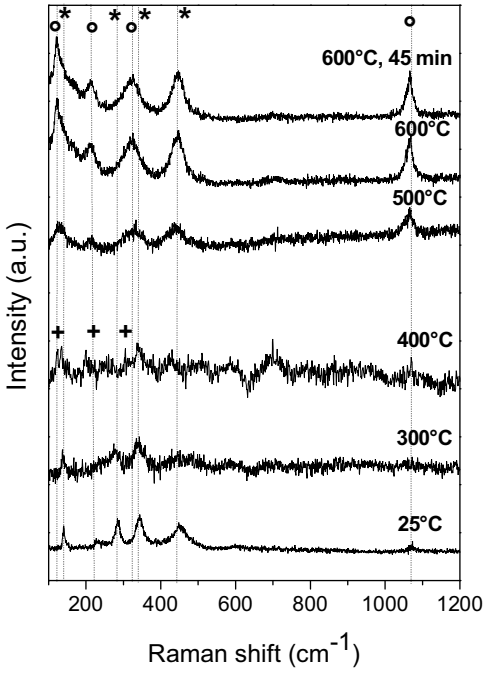

Fig. 9. In situ LRS of Sr5 catalysts under reaction conditions. F = 20 ml/min; 30% CH4, 2% O2 and 68% Ar. (* $La(OH)_3$, ° $La_2O_2CO_3$, +LaOOH).

assigned to the La_2O_3 phase, whereas the weak signal at 1072 cm^{-1} is assigned to $La_2O_2CO_3$ [38–41].

In a preliminary study, the Raman spectra showed the evolution of La_2O_3 phase into $La(OH)_3$ and $La_2O_2CO_3$ for the Sr5 catalyst, after remaining 24 h at atmospheric conditions.

The alumina foam spectrum was similar to the powders spectra but it showed higher intensities, especially for $La_2O_2CO_3$ signals. The spectra of the monolithic catalysts did not show significant differences to the previous ones presented.

The active species of Sr5 catalyst under reaction conditions were studied by in situ Raman Spectroscopy. The spectra at different temperatures are presented in Fig. 9. At 25 °C, $La(OH)_3$ signals at 140, 226, 287, 343, 453 and 603 cm^{-1} could be observed. In addition, a weak band at 1072 cm^{-1} belonging to $La_2O_2CO_3$ was also evident. As the temperature increased, between 300 °C and 400 °C, there appeared new signals at 118, 215 and 323 cm^{-1} corresponding to LaOOH species, while $La(OH)_3$ bands decreased [31]. This lanthanum species was seen at 400 °C by Orera et al. during a thermal evolution of $La(OH)_3$ in air heating at 10 °C/min [42]. It is believed that LaOOH is the intermediate species when $La(OH)_3$ sequentially decomposes into $La_2O_2CO_3$ and La_2O_3. Above 500 °C, when the OCM conversion increased (as described in the following paragraphs), predominant lanthanum phases were $La(OH)_3$ and $La_2O_2CO_3$ generated by the interaction of La_2O_3 with some reaction products (CO_2 and H_2O). After that, the temperature was increased to 600 °C and the spectrum showed the same bands as at 500 °C. Finally, the catalyst was maintained at this temperature during 45 min and no significant changes were observed.

As in our experiments the catalyst follows the same tendency as the catalyst studied by Orera et al., it could be concluded that above 700 °C all lanthanum species decompose into La_2O_3 [42,43]. It was not possible to reach that temperature because of the Raman cell operation limits.

Alexiadis et al. attributed the good activity of the Sr/La_2O_3 catalysts to the stability of surface hydroxyl species [13,44]. However, these species are also related to the formation of chemisorbed atomic oxygen, which in turn negatively affects the C_2 selectivity because it oxidizes both ethylene and ethane reaction products. As indicated above, in our in situ Raman study, the presence of hydroxyl species was corroborated between 400 and 600 °C.

3.5. Catalytic performance

The structured catalysts that showed good mechanical stability ((M)Sr2, (M)Sr5 and (FAl)Sr5) were evaluated for the oxidative methane coupling reaction (OCM). The two foams, (FSiAl)Sr5 and (FZr)Sr5, were not evaluated due to the poor adherence of the washcoats. Coating morphologies previously presented and also adherence tests were useful to discard these two structures.

Methane conversion, selectivity towards ethane + ethylene, towards $CO + CO_2$ and the yield as functions of reaction temperature are presented in Fig. 10. The behavior of powder catalysts, Sr2 and Sr5, is also presented for comparison. Fig. 10(A) shows methane conversion for the five catalysts. The powders showed a maximum conversion of 13% for Sr2 and 17% for Sr5 at 700 °C, and these values were maintained up to 800 °C.

It can be observed that the monoliths showed better performances than the powders, the highest methane conversion value being 34% at 800 °C for (M)Sr5. This value is approximately two times higher than the one corresponding to the powder. Furthermore, (M)Sr2 performance is also better than the one presented by the powder. The foam (FAl)Sr5 presented a similar behavior to its corresponding powder, Sr5.

Selectivity towards ethylene + ethane is presented in Fig. 10(B) for the five different catalysts. The maximum value was around 55% at 750 °C for both powders. In this sense, Sr2 and Sr5 showed similar behaviors. However, the behavior of monoliths ((M)Sr2 and (M)Sr5) was not significantly different from that of the powders, which presented better C_2 selectivity results with a maximum of 65%, at 800 °C. The best selectivity results were shown by the foam. (FAl)Sr5 reached a maximum of 71% at 800 °C. Furthermore, at 500 °C, this foam presented a selectivity value of 57% while that of the monoliths was 33%.

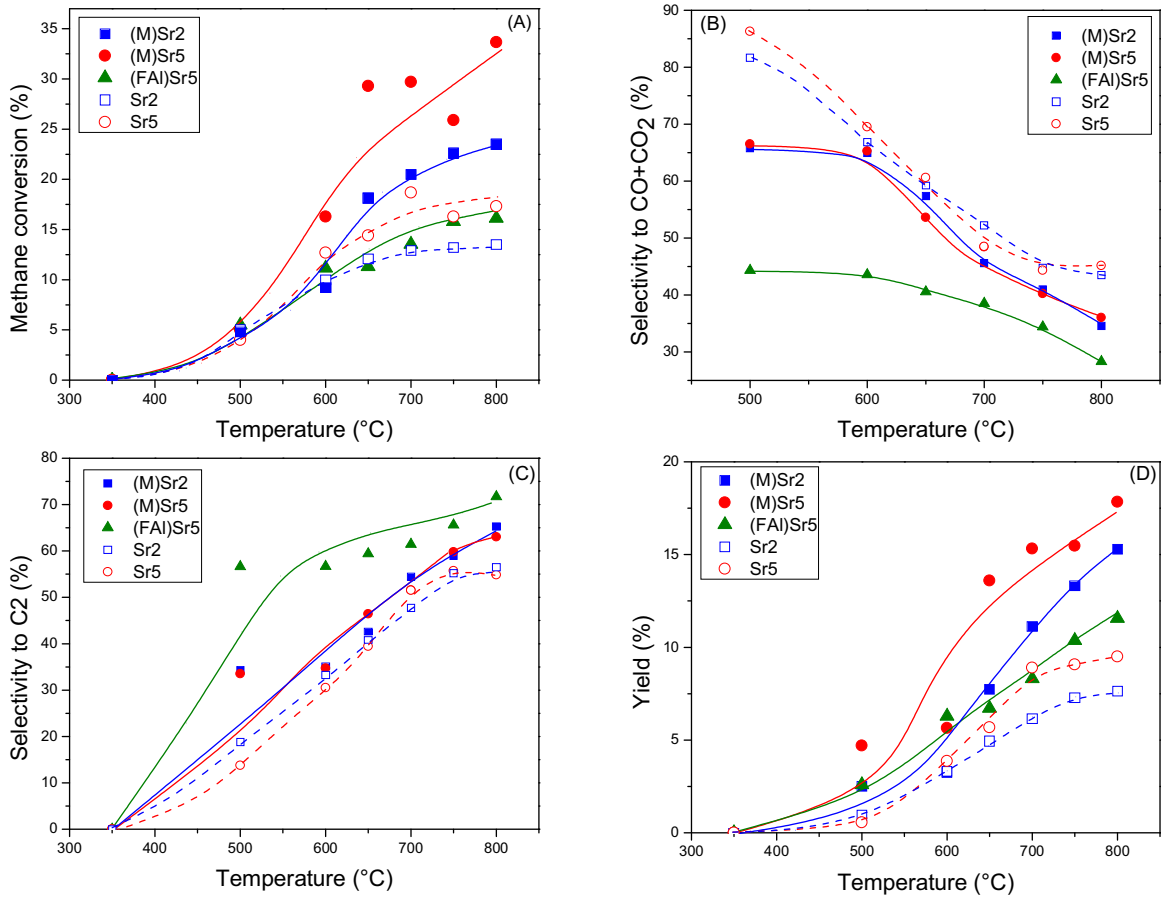

Fig. 10. Catalytic activity of Sr2, Sr5, (M)Sr2, (M)Sr5 and (FA)Sr5. (A) Methane conversion, (B) Selectivity towards $CO+CO_2$, (C) Selectivity towards C_2 and (D) Yield.

Fig. 10(C) shows selectivity towards $CO + CO_2$. These percentages decreased with temperature, reaching a minimum at the highest temperature. Among the structured catalysts studied, (FAl)Sr5 showed the lowest $CO + CO_2$ selectivity values.

Reaction yields are also presented in Fig. 10(C). The Sr5 powder shows a slightly higher yield than Sr2 for the OCM reaction. Therefore, this powder was chosen to coat the foam structures. The maximum yields of 10% and 8% were reached by Sr5 and Sr2, respectively, at 800 °C. The foam, (FAl)Sr5, showed a higher yield, 12% at 800 °C. The best results were obtained for the monolithic catalysts, 15% and 18% at 800 °C for (M)Sr2 and (M)Sr5, respectively.

At 500 °C, the ethylene/ethane ratio is almost null for all the catalysts studied, and it gradually increases when temperature increases. Particularly, in the case of (M)Sr5, ethylene/ethane ratio varied from 0.75 to 2.15 in the temperature range evaluated (600–800 °C).

With these observations, it can be concluded that the use of our catalysts washcoated on cordierite monoliths allows reaching much better OCM performances. This result could be ascribed to the chemical composition of cordierite or to their improved mass transfer properties. Thus, the elements present in the monolithic structure (SiO_2-Al_2O_3-MgO) could interact with catalyst components, which could increase methane conversion, probably by modulating the amount of surface hydroxyl species, as proposed by Alexiadis et al. as a key factor [13,37]. By means of the XPS technique, monoliths showed significant differences in La 3d region with respect to powders. These changes could be due to La environment, which may favor the formation of a well-dispersed lanthanum disilicate phase or because of the presence of MgO. Therefore, Sr(5 wt.%)/$La_2Si_2O_7$ catalyst was prepared and tested for the OCM reaction, showing poor catalytic activity (maximum C_2 yield of 5% at 800 °C). Hence, the higher methane conversion values could be related to the presence of MgO into Sr/La_2O_3 catalysts. MgO can improve Sr(2 or 5) performance owing to its high basicity [20,45,46]. The interaction of cordierite oxides with the active phase was also seen in the O 1 s spectra. The amount of lattice oxygen present in monolithic catalyst was higher than in powders. In addition, migration of cordierite oxides to the catalytic film was evidenced by means of the EDX technique [27,47].

Another important fact related to the improvement of the catalytic activity of monolithic catalysts that was seen by XPS technique was that the relationship of Sr/La in these structured catalysts is lower than in powders and foam. This fact indicates that in monoliths, strontium is well dispersed as it was also confirmed by EDX. When strontium distribution was studied it was noticed that it was homogenously dispersed over the totality of the catalyst, active film and structured support. It is known that the insertion of strontium into the lattice of the host oxide affects its defect structure, and causes the formation of oxygen-anion vacancies [26,27]. This lattice defects are believed to play an important role in the OCM reaction. If strontium is well dispersed into the catalyst it could modify not only La_2O_3 properties but also properties of oxides from the cordierite components like MgO, SiO_2 or Al_2O_3 [48]. The facts discussed above indicate an increase of active sites into the catalyst, and this is related to the higher conversion values reached by the monolithic catalyst.

It should be noticed that due to the monolithic channel dimensions, the partial and/or total oxidation of CH_4 and C_2 to CO or CO_2 is favored. The production of methyl radicals occurs onto the catalyst surface, and they couple themselves in the gas phase, where oxida-

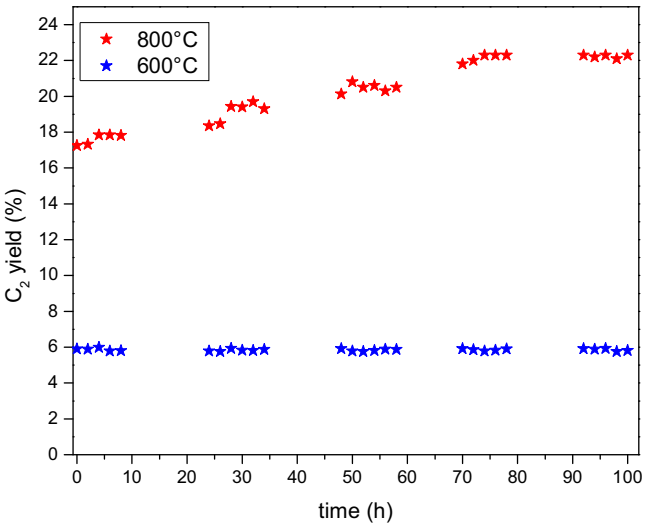

Fig. 11. Catalytic stability tests at 600 and 800 °C over (M)Sr5.

tive reactions take place. If the gas phase/catalytic surface ratio is high, C_2 products and methane are more exposed to be oxidized, disfavoring C_2 selectivity. With respect to alumina foam, it was observed by SEM that it has interconnected pores of small dimensions. Therefore, main products and methane are less exposed to be partially or completely oxidized to CO and CO_2, considerably increasing C_2 selectivity.

In the (FAl)Sr5 catalyst, some chemical interaction between the catalyst components and the structure was seen by XPS but it was not as remarkable as in the case of cordierite, which results in no significant methane conversion increase when compared with the powder. In addition, as it was discussed above, Sr5 spread homogeneously into the micropores of alumina support. Nevertheless, no evidence of Al_2O_3 migration from the substrate to the active catalyst film was observed by the EDX mapping performed over (FAl)Sr5.

3.6. Catalytic stability test and temperature profile over the monolith

In order to evaluate the catalysts stability over the most active system, (M)Sr5, time-on-stream experiments were performed at 600 and 800 °C and the results are shown in Fig. 11. Kondratenko et al. reported a time on stream over La-Sr-based powder catalysts and no changes in the C_2 yield were observed [20]. At 600 °C, in our study of the (M)Sr5 monolith, C_2 yield stayed stable at around 5.8% during 100 h. However, at 800 °C, surprisingly C_2 yield steeply increased from 18% to 22.5% during the first 70 h and then it remained constant until 100 h. This phenomenon could be due to the decomposition of carbonated species (strontium carbonate and lanthanum oxycarbonate) that are unstable at temperatures above 700 °C [43,49]. However, this decomposition takes place in short periods of time; thus, the catalyst activation observed cannot be originated in the said decomposition. Most probably, a gradual increase in the chemical interactions between the cordierite components and the catalytic layer, as suggested above, could be the beneficial effect that improves C_2 yield. Moreover, the constant yield observed at 600 °C in the same period of time-on-stream further validates our hypothesis, because this lower temperature is not enough to provoke the beneficial interactions between the catalytic layer and the cordierite monolith.

In order to study the temperature effect on the OCM reaction, an axial temperature profile was obtained over (M)Sr5. This profile was performed by setting the thermocouple on the monolith center over a hole made between two channels. The measurement instrument was slid through the channels length and temperature values were obtained, showing only small variations. Even though the experiment was not accurate because it modified the gases flow and the thermocouple was in contact with the monolith walls [50], the temperature values obtained suggest the absence of a severe hot spot during the reaction. This could be caused by the low reactant flow and concentrations used in the experiments. Therefore, the heat flux calculated from the reaction enthalpy and the observed methane conversion is low (2.12 W). Anyway, it cannot be claimed that there exists a flat temperature profile due to the limitations of the measurement performed, as pointed out above. Nevertheless, it can be concluded that in general, the heat transference processes are somewhat improved in monoliths as compared with powder catalysts. In our monolithic structure, the catalyst (400 mg) is well dispersed in a bigger reactor volume (2 cm^3) than in the packed powder catalyst (0.7 cm^3), which is favorable for a better heat transfer [51]. However, this point requires further analysis, for example using a theoretical model to predict radial and axial temperature profiles [52,53].

4. Conclusions

Homogeneous and mechanically stable catalytic films were obtained by the washcoating of cordierite monoliths with Sr2 and Sr5, with the addition of silica as binder. However, a very poor mechanical stability was observed when the cordierite monolith was first coated with La_2O_3, followed by Sr impregnation. This could be probably due to acid-base interactions between the lanthana coating and the Sr nitrate solution.

On the other hand, the coated alumina foam showed an adequate porosity which allows this structure to retain the catalyst particles, yielding a homogeneous and stable film. In the case of the other foams studied (aluminum silicate and magnesia-stabilized zirconia foams), the obtained coatings presented very poor adherence.

The catalytic surface XPS characterization of both powders and structured catalysts indicates that La is mainly present as hydroxide and carbonate, and that Sr is mainly present as carbonate. However, in the case of washcoated cordierite monoliths, a modification in the La 3d signal suggests a strong interaction of La with its chemical environment, most probably with silica and/or magnesium. This interaction could be originated by the migration of the components of cordierite towards the catalytic film, as seen by EDX.

By in situ LRS, the decomposition of $La(OH)_3$ and $La_2O_2CO_3$ into La_2O_3 under reaction conditions was confirmed. While hydroxide prevails at low temperature, the presence of oxycarbonates starts to be relevant when the reaction takes place at temperatures above 400 °C and they decompose into the oxide over 700 °C.

It is worth noticing that the monolithic catalysts (M)Sr2 and (M)Sr5 resulted twofold more active towards ethane and ethylene than the corresponding Sr2 and Sr5 powders. Meanwhile, the washcoated foam (FAl)Sr5 showed a similar methane conversion as the powder but higher C_2 selectivity; thus, the C_2 yield was also higher. In the case of the monolithic catalysts, the increase in methane conversion and C_2 yield could be related to La interaction with the silica and/or magnesia present in the cordierite structure.

In the case of the alumina foam catalyst, the higher selectivity could be originated by the lower gas phase/catalytic surface ratio (as compared with the monolith) that prevents the gas-phase combustion of the C_2 products.

The best catalyst among those studied in this work, (M)Sr5 was stable during a time-on stream run at 800 °C. Moreover, the C_2 yield steeply increased from 18% to 22.5% during the first 70 h and then remained constant until 100 h. This phenomenon could be due to

a gradual increase in chemical interactions between the cordierite components and the catalytic coat. At lower temperature (600 °C), the C_2 yield was constant during the 100 h of time-on-stream, indicating that this temperature is not enough to produce the said effect.

Acknowledgments

The authors wish to acknowledge the financial support received from UNL, ANPCyT and CONICET. They are also grateful to ANPCyT for PME Grants to finance the purchase of the characterization equipment. Thanks are given to María Fernanda Mori for the XPS measurements.

References

[1] A. Galadima, O. Muraza, J. Ind. Eng. Chem. 37 (2016) 1–13.
[2] E.E. Wolf, J. Phys. Chem. Lett. 5 (2014) 986–988.
[3] W. Taifan, J. Baltrusaitis, Appl. Catal. A: Gen. 198 (2016) 525–547.
[4] G.E. Keller, M.M. Bhasin, J. Catal. 73 (1982) 9–19.
[5] G.S. Lane, E.E. Wolf, J. Catal. 113 (1988) 144–163.
[6] G.S. Lane, E.E. Miró, E.E. Wolf, J. Catal. 119 (1989) 161–178.
[7] E.E. Miró, Z. Kalenik, J. Santamaria, E.E. Wolf, Catal. Today 6 (1990) 511–518.
[8] Research Institute of Petroleum Industry, US Patent 7,902,113 (2011).
[9] J. Song, Y. Sun, R. Ba, S. Huang, Y. Zhao, J. Zhang, Y. Sun, Y. Zhu, Nanoscale 7 (2015) 2260–2264.
[10] R. Ghose, H.T. Hwang, A. Varma, Appl. Catal. A: Gen. 452 (2013) 147–154.
[11] S.L. González-Cortés, J. Orozco, B. Fontal, Appl. Catal. A: Gen. 213 (2001) 259–271.
[12] J.M. Deboy, R.F. Hicks, J. Catal. 113 (1988) 517–524.
[13] V.I. Alexiadis, J.W. Thybaut, P.N. Kechagiopoulos, M. Chaar, A.C. Van Veen, M. Muhler, G.B. Marin, Appl. Catal. B: Environ. 150–151 (2014) 496–505.
[14] D. Schweer, L. Mleczko, M. Baerns, Catal. Today 21 (1994) 357–369.
[15] S. Pak, J.H. Lunsford, Appl. Catal. A: Gen. 168 (1998) 131–137.
[16] F. Raouf, M. Taghizadeh, M. Yousefi, Int. J. Chem. React. Eng. 12 (2014) 1–9.
[17] T. Zhou, L. Li, J. Cheng, Z. Hao, Ceram. Int. 36 (2010) 529–534.
[18] M.V. Twigg, J.T. Richardson, Chem. Eng. Res. De 80(A (2002) 183–189.
[19] P. Avila, M. Montes, E.E. Miró, Chem. Eng. J. 109 (2005) 11–36.
[20] E.V. Kondratenko, M. Schlüter, M. Baerns, D. Linke, M. Holena, Catal. Sci. Technol. 5 (2015) 1668–1677.
[21] L.E. Gómez, I.S. Tiscornia, A.V. Boix, E.E. Miró, Appl. Catal. A: Gen. 401 (2011) 124–133.
[22] E.D. Banús, V.G. Milt, E.E. Miró, M.A. Ulla, Appl. Catal. B: Environ. 132–133 (2013) 479–486.
[23] E.D. Banús, V.G. Milt, E.E. Miró, M.A. Ulla, Appl. Catal. A: Gen. 362 (2009) 129–138.
[24] O. Sanz, I. Velasco, I. Reyero, I. Legorburua, G. Arzamendi, L.M. Gandía, M. Montes, Catal. Today 27 (2016) 131–139.
[25] G. Gayco, D. Wolf, E.V. Kondratenko, M. Baerns, J. Catal. 178 (1998) 441–449.
[26] H. Borchert, M. Baerns, J. Catal. 168 (1997) 315–320.
[27] U. Zavyalova, M. Holena, R. Schlogl, M. Baerns, ChemCatChem 3 (2011) 1935–1947.
[28] G.R. Gallaher, J.G. Goodwin, C.S. Huang, M. Houalla, J. Catal. 140 (1993) 453–463.
[29] B.M. Faroldi, E.A. Lombardo, L.M. Cornaglia, Appl. Catal. A: Gen. 369 (2009) 15–26.
[30] M.F. Sunding, K. Hadidi, S. Diplas, O.M. Løvvik, T.E. Norby, A.E. Gunnæs, J. Electron Spectrosc. Relat. Phenom. 184 (2011) 399–409.
[31] B.M. Faroldi, J.F. Múnera, L.M. Cornaglia, Appl. Catal. B: Environ. 150–151 (2014) 126–137.
[32] H. Vidal, S. Bernal, R.T. Baker, D. Finol, J.A. Pérez Omil, J.M. Pintado, J.M. Rodríguez-Izquierdo, J. Catal. 183 (1999) 53–62.
[33] M.S. Islam, D.J. Ilett, S.C. Parker, J. Phys. Chem. 98 (1994) 9637–9641.
[34] V.J. Ferreira, P. Tavares, J.L. Figueiredo, J.L. Faria, Catal. Commun. 42 (2013) 50–53.
[35] J.M. Moggia, V.G. Milt, M.A. Ulla, L.M. Cornaglia, Surf. Interface Anal. 35 (2003) 216–225.
[36] M.V. Bukhtiyarova, A.S. Ivanova, L.M. Plyasova, G.S. Litvak, V.A. Rogov, V.V. Kaichev, E.M. Slavinskaya, P.A. Kuznetsov, I.A. Polukhina, Appl. Catal. A: Gen. 357 (2009) 193–205.
[37] A.M. Jastrzębska, E. Karwowska, A.R. Olszyna, A. Kunicki, Surf. Coat. Technol. 271 (2015) 225–233.
[38] S.I. Boldish, W.B. White, Spectrochim. Acta Part A: Mol. Spectrosc. 35 (1979) 1235–1242.
[39] J. Zarembowitch, J. Gouteron, A.M. Lejus, Phys. Stat. Sol. B 94 (1979) 249–256.
[40] C.R. Gopinath, I.D. Brown, J. Raman Spectosc. 12 (1982) 278–280.
[41] S.S. Chan, A.T. Bell, J. Catal. 89 (1984) 433–441.
[42] A. Orera, G. Larraz, M.L. Sanjuán, J. Eur. Ceram. Soc. 33 (2013) 2103–2110.
[43] R.P. Taylor, G.L. Schrader, Ing. Eng. Chem. Res. 30 (1991) 1016–1023.
[44] V.I. Alexiadis, M. Chaar, A. van Veen, M. Muhler, J.W. Thybaut, G.B. Marin, Appl. Catal. B: Eviron. 199 (2016) 252–259.
[45] P. Schwach, W. Frandsen, M.G. Willinger, R. Schlögl, A. Trunschke, J. Catal. 329 (2015) 560–573.
[46] P. Schwach, N. Hamilton, M. Eichelbaum, L. Thum, T. Lunkenbein, R. Schlögl, A. Trunschke, J. Catal. 329 (2015) 574–587.
[47] E.V. Kondratenko, D. Wolf, M. Baerns, Catal. Lett. 58 (1999) 217–223.
[48] D. Filkova, D. Wolf, G. Gayko, M. Baerns, L. Petrov, Appl. Catal. A: Gen. 159 (1997) 33–44.
[49] Z. Stansch, L. Mleczko, M. Baerns, Ind. Eng. Chem. Res. 36 (1997) 2568–2579.
[50] S.T. Kolaczkowski, Catal. Today 47 (1999) 209–218.
[51] A. Cybulski, J.A. Moulijn, Catal. Reviews: Sci. and Eng. 36 (2) (1994) 179–270.
[52] G. Groppi, E. Tronconi, Chem. Eng. Sci. 55 (2000) 2161–2171.
[53] M.L. Rodríguez, L.E. Cadús, D.O. Borio, Chem. Eng. J. 306 (2016) 86–98.